12-2011

Fenestration studies on building energy using the facade evaluation facility

Wendell Cocina
University of Nevada, Las Vegas

FENESTRATION STUDIES ON BUILDING ENERGY USING THE FAÇADE EVALUATION FACILITY

By

Wendell Concina

Bachelor of Science Degree in Mechanical Engineering

University of Nevada, Las Vegas

2009

A thesis submitted in partial fulfillment

of the requirements for the

Master of Science Degree in Mechanical Engineering

Department of Mechanical Engineering

Howard R. Hughes College of Engineering

The Graduate College

University of Nevada, Las Vegas

December 2011

THE GRADUATE COLLEGE

We recommend the thesis prepared under our supervision by

Wendell Concina

entitled

Fenestration Studies on Building Energy Using the Façade Evaluation Facility

be accepted in partial fulfillment of the requirements for the degree of

Master of Science in Mechanical Engineering
Department of Mechanical Engineering

Robert Boehm, Committee Chair

Suresh Sadineni, Committee Member

Yitung Chen, Committee Member

Yahia Baghzouz, Graduate College Representative

Ronald Smith, Ph. D., Vice President for Research and Graduate Studies
and Dean of the Graduate College

December 2011

Abstract

The project was developed to assess several types of facades and their influence on building energy, mainly focused on windows and other building fenestrations. Requirements for the facility are stated in this paper alongside corresponding solutions. The facility is designed to represent a section of a building façade. Experimenting on a wide range of fenestrations including windows with integrated PV elements was the primary prerequisite. The option of removable façade configurations was used and allowed testing specimens to be changed effortlessly. Instrumentation and data acquisition are discussed including calibration and uncertainty analysis. Investigation of the air conditioning unit was concluded during the calibration stage. Fenestration property measurements such as the thermal and optical performance have been evaluated for several windows. Theoretically calculated values and experimental data are compared. Data acquired demonstrate the influence the façade has on the building energy loads. Additional research into these characteristics assists in improving building energy efficiency. Moreover, outcomes of the results are analyzed for residential or commercial purposes, giving practical information for wide-ranging conditions. Further testing of different types of facades will continue and comparisons can be inferred between specimens. Development of the data will help provide valuable information for energy efficient building design.

Acknowledgments

This development was funded by the U.S. Department of Energy, through the Nevada Renewable Energy Consortium (NVREC).

Immense gratitude goes toward Dr. Robert Boehm for the opportunity to work at the Center for Energy Research and his support and patience throughout the process. I would also greatly thank Dr. Suresh Sadineni for his added insight and assistance. As my primary advisors, they provided me with the proper direction and tools necessary to succeed. For these reasons, I am forever indebted to my advisors for their invaluable guidance.

It was a great pleasure to have Dr. Yitung Chen and Dr Yahia Baghzouz as my committee members and appreciate their contributions and guidance not only for me but for the entire Center for Energy Research. Without careful attention to research, progress will be halted. Thank you to the entire UNLV Mechanical Engineering Department staff for making this process a pleasant experience.

Special regards go to Rick Hurt (Research Engineer) and to my fellow colleagues at the Center for Energy Research for their immeasurable aid in the project. I have a great deal of respect for each one of them and thanks for all the knowledge bestowed upon me.

Lastly, thank you to my family and friends for everything they have done. I am very fortunate to have such a supportive cast. Thank you to everyone and I wish you the best on your future endeavors.

Table of Contents

List of Figures

List of Tables

Chapter 1: Introduction

Sustainability and energy efficiency are the prime objectives influencing contemporary energy policies. Several government entities are dedicated to limiting greenhouse gas emissions. The urgency of transitioning to a low-carbon economy is escalating due to climate change. Buildings represent significant amounts of energy consumed, primarily consisting of heating and cooling energy usage [1,2]. Forty percent of United States (U.S.) primary energy utilization is consumed by buildings, which contributes up to thirty-nine percent of the carbon dioxide (CO_2) emissions in the U.S. These buildings also account for seventy-two percent of the total electricity consumption in the U.S. [3]. Residential buildings in the U.S. consume over twenty percent of the annual energy usage [4]. Other nations also exhibit comparable figures. Global contribution towards energy consumption from buildings (residential and commercial) has increased steadily between twenty and forty percent in developed nations, exceeding other major sectors such as industrial and transportation. Population growth, improved standard of living, demand for building services and comfort levels, alongside the upward trend of time spent in buildings assure that the energy demand will continually rise in the future. Due to these facts, it is reiterated that building energy efficiency is an important matter for energy policy at the regional, national and international levels [3,5].

Research directed by the Department of Energy (DOE) to reduce energy usage aids in promoting more energy conscious building designs. A DOE sponsored program set goals to reduce new residential buildings' energy use by seventy percent and provide thirty percent of additional onsite power generation by 2020. Additionally, the program plans to integrate the building's envelope with its mechanical systems for optimal energy savings. The building envelope includes walls, windows, roof and foundation. The mechanical systems include the space/water heating, cooling and ventilation. This essentially turns the façade into a multifunctional system that plays a major role in building energy [4].

The significance of facades toward energy efficiency and sustainability is exemplified by advancements of facades touted as high-performance commercial building facades. Several technological techniques and designs for high performance façades are based on central concepts such as space conditioning, ventilation, daylighting, and solar heat gain control. One method of solar heat gain control can be accomplished through the use of spectrally selective glazing which permits certain portions of the solar spectrum to transmit through the window and into the building while rejecting any undesired portions. Daylighting is provided while decreasing solar heat gain, thus reducing building energy consumption and peak demand. Warm and cold climates can benefit from this technology because of its solar radiation transmission properties and can be applied to residential or commercial buildings. Additional solar control window technologies include angular selective control, solar filters and exterior solar control. Natural ventilation and double skin facades use a second layer for heat recovery during cold winters and heat extraction

during the summer. This offers the opportunity to utilize an all-glass façade for aesthetically desirable arrangements while providing natural ventilation. Vacancy in the cavity of the double-skin façade can be taken advantage of by implementing a shading apparatus. Active facades provide dynamic fine-tuning of optical and thermal properties in response to climate, occupant preferences, and building energy management control system requirements. With the combination of these concepts, improved indoor air quality, enhanced energy efficiency, thermal comfort and occupant performance can be achieved. Moreover, downsized mechanical equipment capacity requirements and reduced operating costs for building owners are achieved [6]. Along with glazing, the building envelope also plays a vital role in energy efficient design. This is especially true in hot and dry climates where a building envelope of greater thermal mass can deliver a greater time lag for the transmission of outdoor temperature into the conditioned space. Careful attention must be considered while applying appropriate strategies for each unique climate since varying degrees of performance and benefits are realized [1].

An important part of a façade is the glazing component. Emerging glazing technologies include: insulation-filled glazing, evacuated windows, building integrated photovoltaics (BIPV), and smart windows (photochromics, thermochromics, liquid crystal device windows, suspended particle device windows, electrochromic windows, gasochromic windows, motorized shading) [7].

Insulation-filled glazing has several options such as aerogel, honeycombs, and capillary tubes between glazing panes. This type of glazing provides diffuse light and is less transparent than standard window glazing. Aerogel is used to prevent convection since the material can entrap air while still allowing light to pass. Conduction is also reduced since the cell sizes are smaller than the mean free path of the air. Long-wave thermal radiation is also virtually eliminated due to the multiple cell walls where the radiation is absorbed and reradiated. Evacuated windows contain no gas in the gaps between the panes. No convective or conductive heat transfer will occur between the glass panes when the vacuum pressure is low enough. The main drawback of this type of window is its structural integrity since it needs to withstand the normal air pressure and variable pressures from sources of wind and vibration. It must also handle large thermal stresses [7].

Smart windows are considered multi-functional and may provide added utility. These facades can have active and passive features. Reduced energy usage and increased comfort are some of the benefits of these facades. Passive devices include photochromics and thermochromics. Active devices include liquid crystal, suspended particle and electrochromics. Photochromic materials adjust transparency according to the intensity of light. These materials dim when exposed to bright light and become transparent when minimal light is present. Thermochromics have variation in transparency in response to temperature. Liquid crystal device windows serve as a privacy glazing. It can scatter light and create a translucent layer, and when power is applied the glazing can become

transparent. Suspended particle device windows act similarly to the liquid crystal. Of the switchable technologies, electrochromic windows are the most promising. It has a great range in adjustable transmission. Gasochromic windows provide a similar effect as electrochromic windows [7].

Building integrated photovoltaic cells can provide electricity generation to augment the building energy usage. Photovoltaic (PV) cells can be integrated within a double skin façade. Ventilation on the rear side of the PV can lower operating temperatures and prevent overheating. Benefits to this technique include increased cell efficiency and waste heat recovery. Optimized percentage of the transparent window and opaque PV can provide balanced daylighting with maximized electricity generation depending on the situation. Many variables such as the climate, room depth, lighting loads, U-value, glazing type, and the shading device are encompassed in this evaluation. Photovoltaic cells can be incorporated into numerous innovative designs that can lead to improved performance [8–11]. Aside from the energy efficiency standpoint, façades provide multiple purposes and can serve as a weather shield, a fire retardant, a source of lighting, a power generation source, and a ventilation source for heating and cooling [9].

The perceived economic benefits for energy efficient buildings include decreased operating costs by nine percent, increased building value by seven and half percent, an improved return on investment by about six percent and an increase in occupancy ratio by three and half percent [12]. Benefits of energy saving measures are also highly regarded

by the consumer with the energy saving benefits, environmental benefits, and comfort benefits attributing to the positive opinion [13].

Due to the complexity of facades, each specific façade component and concept should be quantitatively evaluated in order to provide performance insights for the building designers. Providing information on different facades and concepts will aid in overall energy efficient building design [6]. For this reason, the Façade Evaluation Facility (FEF) was developed. The Façade Evaluation Facility (FEF) was developed to assess façade components and provide insight on the overall performance of different façades based on the thermal and solar characteristics exhibited from testing.

Chapter 2: Literature Review

2.1 Theoretical Window Analysis

Window fenestration programs and simulations were used to theoretically determine the U-Value and Solar Heat Gain Coefficient (SHGC) of glazing. A popular publically available computer code used for heat transfer analysis using methods consistent with the updated rating procedure developed by the National Fenestration Rating Council (NFRC) that is consistent with the ISO 15099 standard is called WINDOW and was developed by the Lawrence Berkeley National Laboratory (LBL) [14]. Pane spacing analysis in glazing systems was completed using computer calculations and compared experimentally [15]. Triple paned window computer analysis was accomplished and optimum spacing and gases were determined, although the analysis had no experimental method to verify the U-factor [16]. Other types of glazing such as switchable glazing were also analyzed using computer model programs for calculating the thermal and optical performance parameters. The performance of the differing solar transmittance spectra, differences of switching from transmission to reflecting versus transmitting to absorbing, and the effects of position of the switchable glazing in a window were examined [17].

2.2 Window Structural Analysis

Stresses on the structure of the window units can result from temperature and pressure differences experienced by the window. Multiple gap designs allow for pressure equilibrium between the gas spaces. This significantly alleviates stresses on the exterior glazing and eliminates pressure loading in the middle layer. This also helps lessen the maximum deflection the unit will experience [18]. Research on triple paned windows and their structural design was conducted for non-standard designs to encourage the use of triple pane windows and shows promise but still requires further investigation [19]. Small and large-scale tests revealing the window breakage characteristics of different glazing samples were performed, including the amount of radiant transmission of energy through the window. Necessary information is provided by the tests to evaluate the hazards of radiant energy such as a fire in near proximity to exterior windows to building occupants and contents. Triple pane windows had lower total transmittance, lower back-side temperatures and heat flux than that of double-pane windows [20].

2.3 Economic Analysis

Other studies included the research on the environmental impact of advanced windows and their global environmental impact. This included a life cycle assessment analysis of the glazing system production, maintenance phase and a thermal balance of its utilization phase. Cradle-to-grave analysis was completed. It has been proven that the most benefit

is gained during the utilization phase, significantly negating any slight increase in production cost and environmental impact [21].

2.4 Window Laboratory Testing

Many window studies were performed using hot boxes to simulate different operating conditions. An experiment determining the U-factor of a window with a long-wave high-reflectivity venetian blind was completed by Fang. The tests were performed in a guarded hot box configuration in accordance to the American Society of Testing and Materials standards (ASTM). Two similar hot boxes were constructed and tested simultaneously for a single and double pane window. The venetian blinds were tested at several angles. An equation for the U-factor with corrections for wind velocity and to account for a window frame was produced to provide estimated values. It was shown that the highly reflective blinds can enhance the thermal insulation performance of the window by adjusting the slat angle [22]. Another test using the same hot box configuration and windows was conducted but with a curtain cloth. Two types of curtain cloths were tested, where one was a dark colored thick cloth and the other being a light colored thin cloth. The effects of cloth materials on window U-factors were studied. The U-factors can be calculated using the experimental results and equations developed for the respective windows with a given cloth curtain. These studies present fenestration results but the values do not

represent field test data and require the use of correction factors to determine performance under realistic conditions [23].

2.5 Facade Testing Facilities

A Mobile Window Thermal Test (MoWiTT) facility was produced that measured the net heat transfer through two window systems simultaneously [24]. The test facility was initially developed to confirm the net energy performance estimations of fenestrations and other complex elements of the building envelope [25]. Previous measurements of fenestration characteristics were often calculations of instantaneous net energy performance at certain design conditions. This method lacked quantitative estimates of the energy consumption to help produce a cost benefit analysis. Also many tests are performed in laboratory settings as described earlier. Field data would be beneficial. Other disadvantages include fundamental errors discussed in the paper. For these reasons the construction of the facility was under consideration. Initially, the best approach in the design of the facility was determined to be a small test room where different fenestrations can be mounted. Accurate measurements of the energy balance within the facility and interior temperature control were early design requirements [25].

Further discussion on the several preceding methods of fenestration characteristic measurements were established in a continuing paper [26]. Previous ways included the “field test” approach where windows are tested in actual buildings and the energy inputs

are used in an energy simulation to provide the necessary results. Another method used was a construction of a simplified test room where the fenestration is mounted. From the energy input measurements, the net heat balance is concluded. These tests however do not provide conclusive behavior on fenestration performance. These reasons demonstrate the need for a facility specially designed for measuring the net energy performance. Designing the facility required sources of error to be identified as well as the need to produce sufficient quality data to provide conclusive answers on fenestration performance. Energy efficient strategies employed in buildings yields smaller differences in heat transfer, thus requiring high accuracy measurements. Several other topics regarding error in sample buildings, limitations of field measurements and error for a passive test cell justified the need for a specialized facility for measuring fenestration energy flow.

The MoWiTT facility was built from the requirements stated earlier and was located at Lawrence Berkeley Laboratory. It consisted of multiple mobile measurement modules, with a centralized instrumentation van used to collect data. Each individual module contains a pair of identical test rooms, each with one removable exterior wall and roof panel. Direct comparative measurements between the fenestration systems exposed to in the same weather conditions can be applied. The MoWiTT also had the capability to relocate to different sites to expose the system to climates of interest. Realistic test conditions are achieved using similar dimensions and materials of a typical building. Measurement accuracy was examined for the instrumentations used [26].

Results from the MoWiTT are described in several papers [24,27]. Measurements are in good agreement with computational program calculations. It was found that uncertainties in thermal performance from solar gain effects overshadow the effects of improved U-value. Also, the paper states there is still a need for improved methods for accounting solar gain effects in windows performance comparisons to properly determine the overall U-value benefits. With no method for treating thermal losses and solar gains, fenestration energy calculations will remain uncertain [24].

The Passive Solar Components and Systems Testing Project (PASSYS) is located on the site of the Building Research Establishment's (BRE) Scottish laboratory in east Kilbride, near Glasgow. It was constructed to determine the performance characteristics of a window utilizing pre-heat background room ventilation. It consists of two heavily insulated rooms with one being a test space and the other as a service room. The south wall can accommodate the various passive solar components. The test cell was compared with a theoretical model of heat transfer within the window. Clarification of the effect of cavity width, ventilation rates, and low-e coating location were intended in the results [28–30].

More recently, a test facility named the Testing Window Innovative Systems (TWINS) was developed at the Department of Energetics at the Politecnico di Torino [31]. The facility consists of two separate identical outdoor cells, where one is used as a reference and the other houses different façade configurations. Field measurements of different

facades were completed, with the indoor conditions controlled. The façade configurations were evaluated after a measurement campaign, which contained a mechanically ventilated air gap and venetian blinds. Performance of the façades was evaluated and currently the active façade is not recommended over opaque facades until further improvements are attained [31].

Chapter 3: Development of Facility

3.1 Fundamental Requirements

Initial design requirements were established for the FEF and approaches to satisfy those requirements then proceeded. Physical unit requirements and experimental data requirements are presented in separate sections and solutions are discussed.

3.1.1 Physical Unit Requirements

Location of the experimentation site is handled outdoors. Since outdoor field testing is necessary, the structure should be weatherproof. A steel shipping container was the most appropriate candidate for this prerequisite. The structure is prebuilt and readily available. When the façade is not in evaluation, protection of the unit should be provided. It was decided that the opening to the main front doors should house the façade specimens, thus allowing the doors to enclose and protect the contents within, during idle periods. Clearance for the façade is taken into account. Because the opening for the main entry doors accommodated the façade, a secondary means of entry was needed. Installation of a personnel door thus provided access within the facility and its contents.

Due to outdoor exposure of solar radiation and high ambient temperature conditions, insulation is essential in minimizing heat transfers within the facility through the walls during summer periods. Calculation of an optimal insulation thickness was concluded. Several varieties and dimensions of façade configurations are planned which require a method of quick interchangeability during testing. In this case, each type of window is installed in a structurally supported slab of insulation and can be placed into and removed from the facility in a short period of time. Adjustment of orientation was also a fundamental requirement. To fulfill this condition, a carousel can be installed underneath the facility allowing manipulation of the orientation without difficulty.

With the physical design requirements addressed, a three-dimensional computer model was rendered with SolidWorks. The subsequent figures exhibit the solutions to each condition. An example of a façade specimen installed into the FEF is illustrated in Figure 1. This particular façade is double pane glazing. Figure 2 shows a rough representation of the carousel including the personnel door placement located on the rear side of the facility.

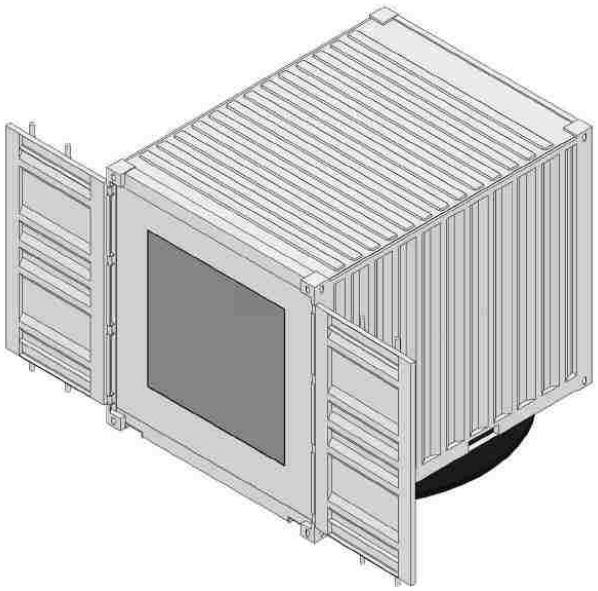

Figure 1 - 3D Model Representation of the Façade Evaluation Facility with Double Pane Glazing Facade

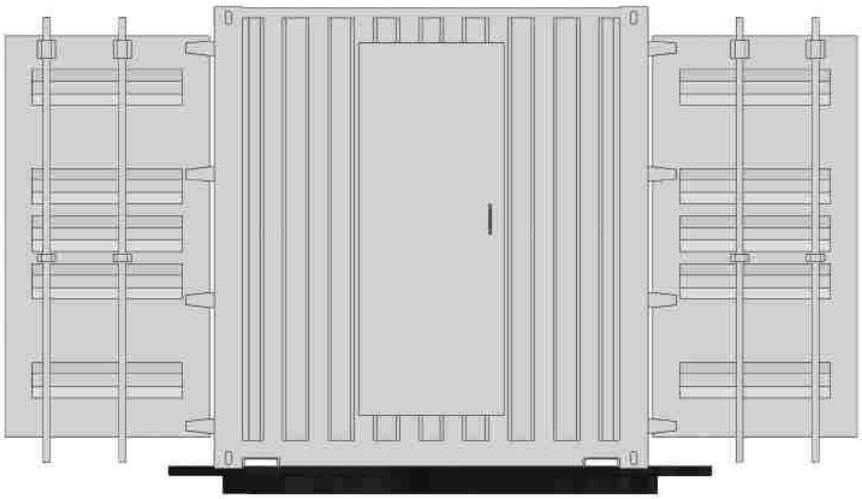

Figure 2 - 3D Model Representation of the Façade Evaluation Facility with Carousel and Personnel Door Placement

3.1.2 Experimental Data Requirements

Experimental data requirements for the FEF primarily entailed sensors of several types and data logging equipment. Interior temperature control was also essential. Temperature control within the facility is fundamental in replicating typical building settings. Moreover, modest temperature differences between the interior and exterior of the façade may yield limited and uncertain data for analysis. Significant temperature differences between the façade interior and exterior can be generated with an air conditioner (AC) system. A mini split ductless AC system was proposed. Although while increased temperature difference between the façade interior and exterior is beneficial for data, the temperature difference also exists between the interior and exterior walls which is unfavorable as it increases the amount of heat transfer through the walls. This displays the importance of proper insulation.

Measurement of meteorological data is required to provide the ambient conditions of the testing location. Ambient temperature probes, pyranometers and a wind sentry were housed in a weather station located adjacent to the FEF. Global horizontal irradiation, ambient temperature, wind speed and wind direction are measured using these meteorological sensors.

Solar irradiance measurement sensors required were a precision spectral pyranometer and multiple standard pyranometers. The pyranometers measured the solar radiation hitting the plane of the façade as well as the solar radiation transmitted through the facade. These

sensors are utilized to determine the optical fenestration characteristics of the facade. Temperature probes, thermocouples, and heat flux sensors were required to measure the temperature and heat flux throughout the facility. Primarily, heat gain through the façade and walls of the unit are evaluated. These are all required to perform an energy balance of the facility. Relative humidity and interior temperature data are also required measurements.

Energy measurement sensors included a combination of Wattnodes® and current transformers. Assessment of the energy consumption wass predominantly focused on the AC unit. The data acquisition system consists of a datalogger and multiplexers placed in an enclosure with a battery power supply for uninterrupted data. Data from all the sensors previously mentioned are stored every minute and scanned every fifteen seconds. The internal loads produced by the data acquisition equipment are considered negligible. From the requirements discussed, a detailed list of accruement was assembled. Major components are summarized in the tables below.

Table 1 – Major Structural and Temperature Control Components

Item	Description
Steel Container	Standard steel storage container 10’x8’x8.5’ (LxWxH)
Carousel	Custom-built carousel for adjusting facility orientation
AC System	Mini split ductless AC system for temperature control (1 ton)

Table 2 – Major Relevant Measurement Sensors

Item	Manufacturer Part	Description
Ambient Temperature Probe	Campbell Scientific 107-L40	Temperature probe for outdoor ambient temperature measurements (Range of -35°C to +50°C)
Pyranometer	Campbell Scientific LI200X-L40	Pyranometer for global horizontal irradiance measurements
Wind Sentry	R.M. Young 03002-LS12-LD12	Wind speed sensor and wind direction sensor for ambient wind conditions
Precision spectral Pyranometer	Eppley Laboratoy, PSP	Precision spectral pyranometer and standard pyranometers used for solar radiation measurements on the façade
Wattnodes®	Continental Control Syst. WNB-3Y-208-P	True RMS AC watt-hour transducer with pulse output (solid state relay closure) proportional to kWH consumed. Used to determine the energy consumption of the AC unit
Current Transformers	Continental Control Syst.CTS-0750-yyy	Split core CTs with removable section, so that they can be installed without interrupting the circuit, used in conjunction with the wattnode. Rated Amps 30
Temperature Probe	Campbell Scientific 108-L60	Temperature probe for interior temperature measurements (-5°C to +95°C)
Thermocouples	Omega Engineering 5TC-TT-K-20-72	Thermocouples for interior surface wall temperatures, type K calibration
Heat Flux Sensors	Omega Engineering HFS-4	Heat flux sensor for precise measurement of heat loss or gain on any surface.

Table 3 – Major Data Acquisition Components

Item	Manufacturer Part	Description
Datalogger	Campbell Scientific CR1000-ST-SW-NC	Measurement and control module to acquire and log data from the measurement devices. 16 single-ended or 8 differential channels, two pulse counters, three excitation channels, and eight control ports. 4 MB SRAM for data storage, program storage and CPU usage.
Analog Channel Multiplexer	Campbell Scientific AM16/32B-ST-SW	16 or 32 Channel Relay Multiplexer. Provides additional measurement ports for data acquisition.
Switch Closure Module	Campbell Scientific SDM-SW8A-SW	8-Channel Switch Closure Input Module. Provides additional measurement ports for data acquisition.
Enclosure	Campbell Scientific ENC16/18-DC-NM	Weather resistant enclosure (16" x 18") with two conduit openings
Power Supply	Campbell Scientific PS100-SW	12V power supply w/ charging regulator and 7Ahr sealed rechargeable battery

3.2 Preparation and Installation

Planning of the location and installation proceeded after the list of accruement was prepared and each item was received.

3.2.1 Preparation

A suitable location for the facility was determined after shading was investigated to ensure that minimal shadows would be cast on the facility by obstructions during testing. The charts displaying the possibilities of shading throughout the year on a south facing facade are shown in Figure 3 and Figure 4 using sun charts provided by the University of Oregon Solar Radiation Monitoring Laboratory at the specified coordinate location [32]. Figure 3 specifically portrays the shading for the first half of the year while Figure 4 is the second half of the year. A long fence and plants are located directly in front of the facility; the amount of shading by obstructions at thirteen feet away is shown on the figures. This distance was deemed too close since shading would occur for up to 8:00 am during morning hours and continue again as early as 3:30 pm during the afternoons for several months of the year. A distance of twenty-one feet away from the fences was then analyzed and represented on the figures. This was chosen as the proper distance away from the fence. The appropriate distance between building obstructions was determined and shading of these obstructions are shown on the charts. The shading analysis is referenced at the extreme points of shading which is most likely to occur at the lowest portion of the possible façade configuration. Adjacent building shading is also shown when the facility is placed at a distance of 21 feet away from the fence.

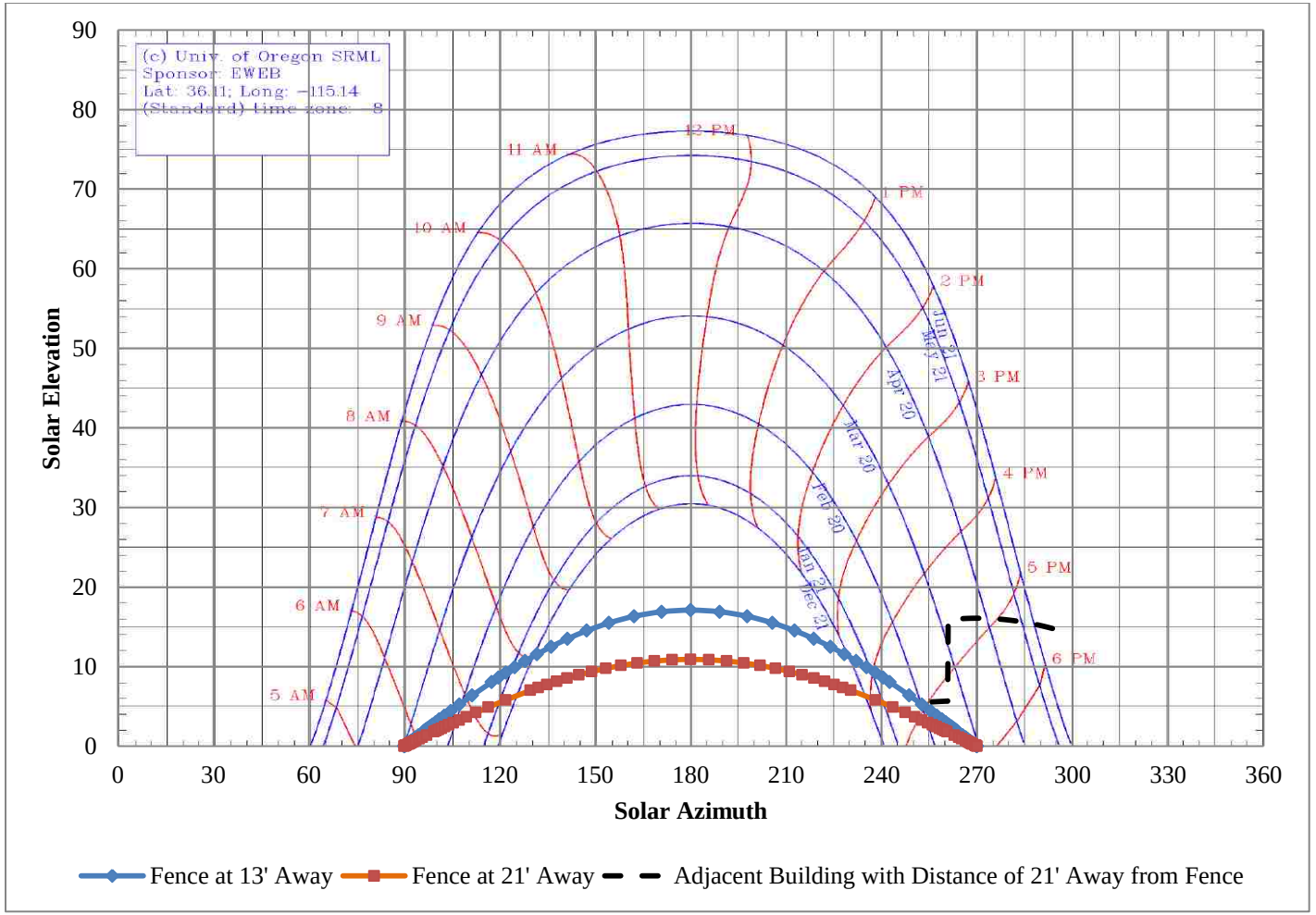

Figure 3 - Shading Analysis First Half of the Year

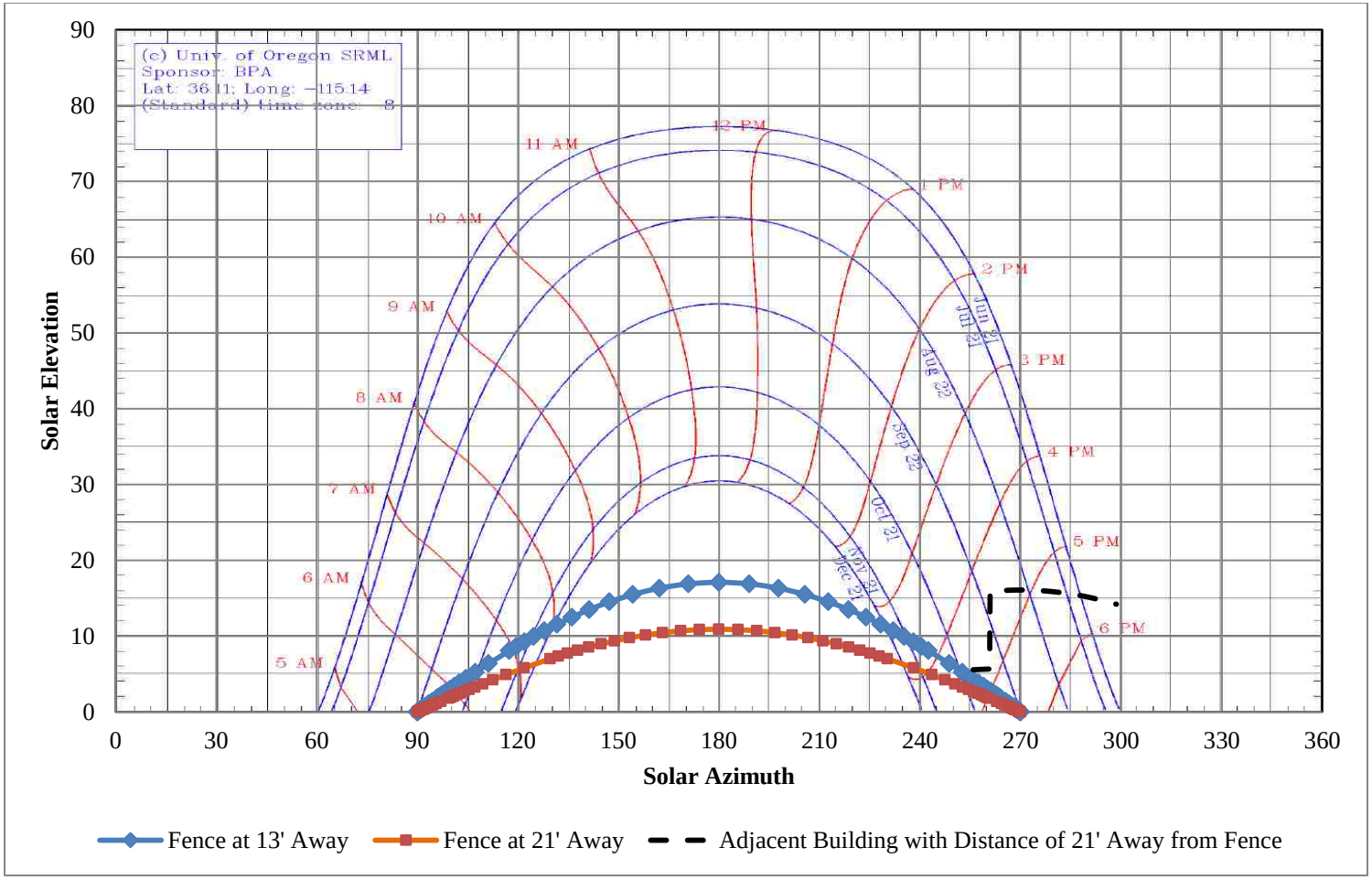

Figure 4 - Shading Analysis Second Half of the Year

A weather station was setup on an adjacent building in close proximity to the FEF to collect the meteorological data at the location. The weather station provides irradiance data in the form of global horizontal, direct normal, diffuse horizontal summarized in Table 4. Meteorological data include the ambient dry bulb temperature, wind speed and direction, summarized in Table 5 [33,34].

Table 4 – Weather Station Irradiance Data

Irradiance Measurement	Unit	Description
Global Horizontal	W/m^2	Total Hemispheric shortwave irradiance as measured by an Kipp & Zonen Model CM3 Pyranometer with calibration factor traceable to the World Radiometric Reference (WRR).
Direct Normal	W/m^2	Direct (Beam) shortwave irradiance as measured by an Eppley Laboratory, Inc. Model NIP (Normal Incidence Pyrheliometer) mounted in an automatic sun-following tracker, with calibration factor traceable to the WRR. The estimated broadband Aerosol Optical Depth (AOD) is also calculated using this instrument.
Diffuse Normal	W/m^2	Diffuse (Sky) shortwave irradiance is calculated using the formula: Global = Direct * Cosine(Zenith) + Diffuse.

Table 5 – Weather Station Meteorological Data

Meteorological Measurement	Unit	Description
Dry Bulb Temperature	^{o}C	Ambient air temperature measured with an RM Young 1000 Ohm 4-Wire RTD inside in a naturally aspirated radiation shield mounted on a pole at approximately 30 feet above ground. The wind chill temperature is also calculated using the new National Weather Service (NWS) method as described on the NOAA web site, however the wind speed used is measured at approx. 30' instead of the 5' level required by the NWS calculation.
Wind Speed and Wind Direction	m/s	Measured by an RM Young 4-blade propeller and attached vane mounted on a pole at approximately 30 feet above ground. Peak Wind Speed is also recorded, which is the maximum 1-sec anemometer reading during the 1-minute interval.

The proper insulation thickness was determined after calculations were made, shown in Figure 8, in order to reduce heat gain from each wall of the container. Insulation calculation was conducted for the hottest day during the summer of previous years to present the most extreme differences between the walls and windows. Summer sun altitudes in Las Vegas, Nevada are very high so the amount of solar radiation transmitted through a south facing window is less than that during winter when the sun is at lower angles. Methods and weather information described by American Society of Heating Refrigerating and Air-Conditioning Engineers (ASRHAE) and other widely available textbooks were used for the calculation [35–37]. The approach was similar and more elementary to an analytical model discussed in a later chapter. A plot of the wall insulation thickness vs. the heat gain factor (HGF) (defined

as the ratio between the heat gain through walls versus the windows) is shown in Figure 5. As shown in the figure, as the insulation values increases the HGF decreases. However, the decrease in HGF had reduced significance beyond an R-value of 40. Styrofoam insulation sheets totaling a thickness of 10 inches and an R-value of 40 were used. The insulation ensured in reducing heat gain experienced through the walls but in the extreme case, wall heat gain plays a major role in overall energy transfer within the facility.

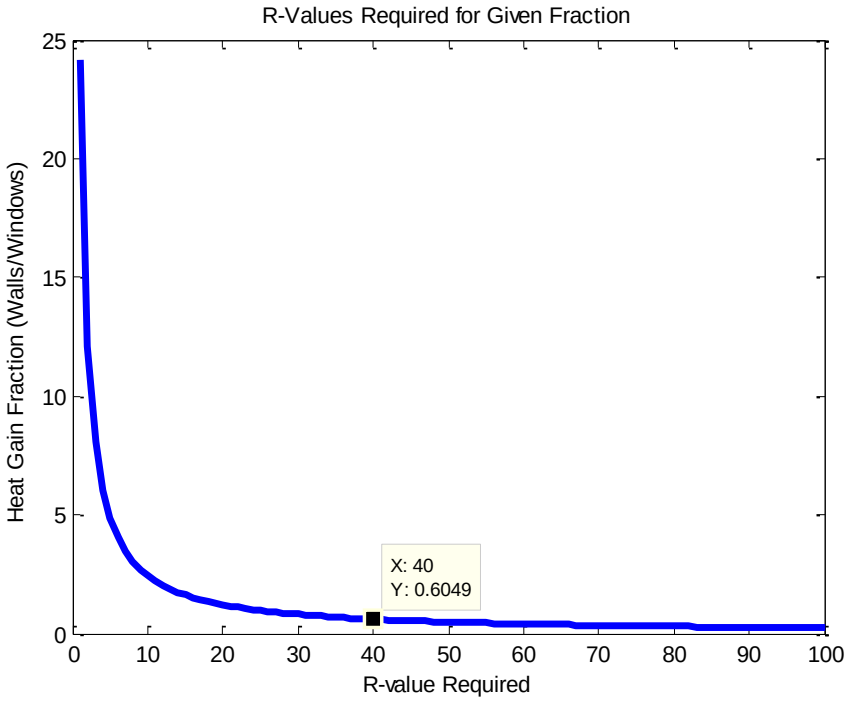

Figure 5 - R-Value Required for Given Heat Gain Fraction

3.2.2 Installation

For the base structure, a steel shipping container shown in Figure 6 was used to handle the outdoor weather conditions and for its durability. The container dimensions are 8.5ft (2.6m) in height, 8ft (2.4m) wide, and 10ft (3m) long. The figure displays the facility at the chosen outdoor location, which is at the Center for Energy Research at the University of Nevada, Las Vegas [38]. The figure also shows the facility in its closed position, protecting the façade and the equipment inside.

The carousel located underneath the facility was attached to the unit allowing the orientation of the FEF to be set to desired testing conditions. The system is oriented to due south as the default test setup since for vertical surfaces, the south orientation (for northern hemispheres) experiences the most direct radiation over the course of entire day. Rotation of the shipping container can be managed by a single person and can be locked into place to prevent undesired rotation due to wind loads. Electrical power for the FEF is located outside of the facility and is led into the facility through a single cable. The provided electricity is used for the sensors, instrumentation, data logging, and most importantly the air conditioning system.

Figure 6 - Façade Evaluation Facility (Closed Position) Location and Setup

The next step of installation was insulating the facility. An optimal insulation thickness of 10 inches (0.254 m) of polystyrene insulation was concluded and applied inside the unit. Eliminating infiltration was an important criterion; therefore air-tight fitting of the insulation was essential. To accomplish this goal the insulation was staggered to eliminate the existence of any continuous seams from the exterior into the interior. Insulation was installed inside the shipping container as shown in Figure 7. From the figure, the staggered arrangement of the insulation can be seen.

Figure 7 - Insulation Installation in the Facility

The same staggered configuration exists in the insulation wall that fits into the opening of the facility that houses the façade; this is shown in Figure 8. A well-fitted insulation plug is fitted into the opening. The figure shows a fully insulated setup where all faces of the container are insulated for calibration purposes when no façade is present.

Figure 8 - Fully Insulated Test Setup

Since the main doors accommodated the façade, a secondary personnel door located on the opposite side was installed. Access inside the facility is possible with the personnel door depicted in Figure 9. The personnel door is sealed with an insulation plug similar to the main door. Notice the staggered appearance of both the plug and the entry door. They are made to fit together to prevent air infiltration as stated for the main doors.

Figure 9 - Personnel Door and Air-Tight Staggered Insulation Plug

Following the insulation installation, electrical and data logging equipment were installed. Figure 10 displays the electrical source found outside of the facility on the left, with the lighting, interior electrical components and data acquisition equipment shown on the right.

Figure 10 - Electrical and Data Logging Components

Interior climate control was achieved by installing a mini-split ductless air conditioning system. Figure 11 displays the interior air handler on the top with the corresponding condenser unit located outside of the container shown on the bottom of the figure. Separating the outdoor compressor/condenser and indoor air-handling unit allows for reduced infiltration. Only a small single penetration was required through the wall of the facility for A/C purposes, thus reducing energy transfers from undesired sources.

Figure 11 - Mini Split Ductless A/C System

Temperature probes, relative humidity and heat flux sensors were installed within the facility. Heat flux sensors were placed in various faces of the facility to properly determine the amount of heat transfer that is experienced throughout. Ambient temperature as well as relative humidity is recorded with the sensors located at the center of container, suspended in air. These sensors are shown in Figure 12.

Figure 12 - RH, Temperature and Heat Flux Sensors (Pictured from left to right)

Figure 13 shows the installation of the precision spectral pyranometer located behind a double pane window to measure transmitted solar radiation.

Figure 13 - Precision Spectral Pyranometer

Current transformers and Wattnodes® were installed to measure the energy the air conditioning unit draws. Figure 14 displays the installation of the sensors into the datalogger. The figure also shows how a computer interfaces with the data acquisition system. After the data is collected, data analysis can begin.

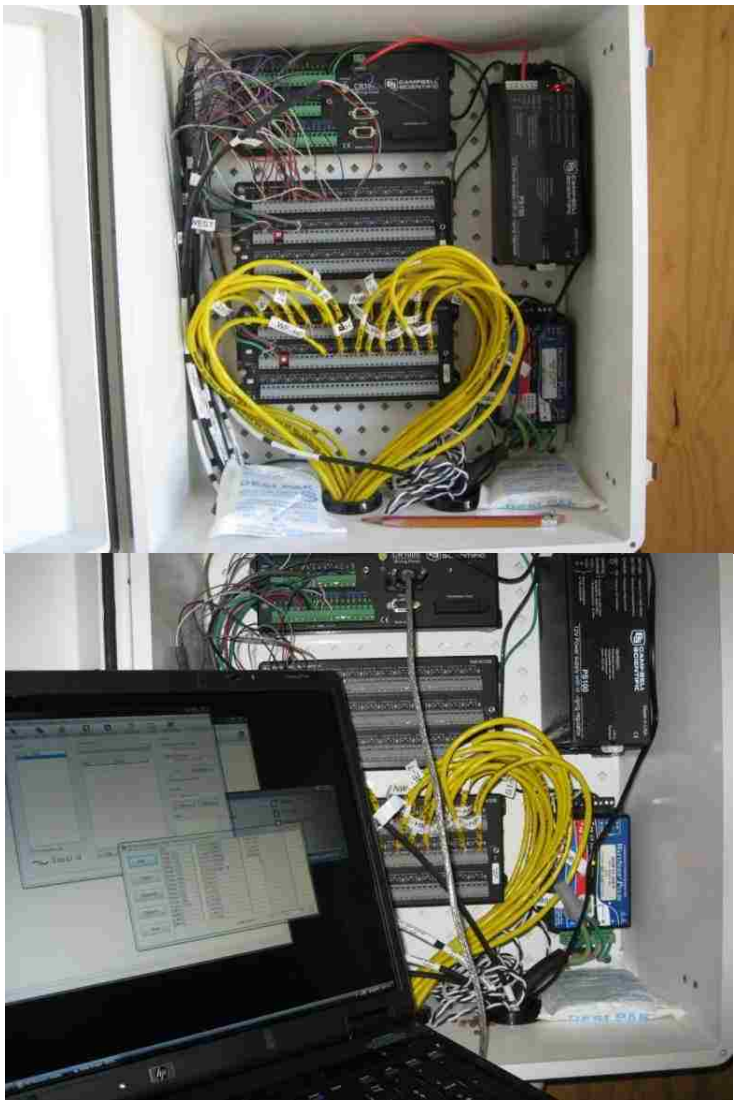

Figure 14 - Sensors Connected to the Datalogger and Interfacing with a Computer

Facades that are transparent (windows) as well as opaque portions of the façade (exterior wall/cladding) are primarily considered for evaluation in the FEF. The facility is a complete standalone unit designed to represent a section of a building façade. Measured results can include fenestration properties such as thermal and optical properties of the windows. The data can show the influence the façade has on the building energy loads.

The ability to change the façade was the main goal of the facility to allow for evaluation of numerous types and sizes of façade configurations. To allow for this, a method of interchangeability was developed. For each type of facade element of interest, a structurally supported slab of insulation was created to accommodate the placement of the item. This is then inserted into the container and can be removed for other types at any given time as depicted in Figure 15, which shows from left to right: no facade, a fully insulated test setup for calibration purposes, and a double pane window setup for baseline testing.

Figure 15 - Facade Interchangeability

Chapter 4: Methodology

4.1 Test methodology

To summarize the description of experiment and methodology, temperature control within the unit is fundamental in reproducing standard building conditions. This allows for a better representation of façade element characteristics for its applicable purposes since varying temperature difference between the indoor and outdoor conditions allows for enhanced understanding of the data and characteristics. Ambient temperature, global horizontal, direct normal solar radiation, wind speed and wind direction are measured at the location. The interior walls, including the floor and ceiling, have heat flux sensors placed on each surface. When a window is being evaluated, heat flux sensors are attached to the glazing and window frame. Several pyranometers and a precision spectral pyranometer measured the transmitted radiation through the window. Appropriate radiation shielding was used when considering heat flux sensors exposed to solar radiation. Surface temperature is also measured with the type-K thermocouples that are attached to the heat flux sensors. In order to observe potential stratification of the environmental temperature inside the facility, three temperature probes at evenly spaced heights are held in the air at the center of the unit. A relative humidity sensor is also suspended at the center of the unit. These measurement sensors will examine changes in the interior conditions of the facility.

Energy transfer within the building can be correlated with the amount of energy consumed by the air conditioner. Accurate measurements of air conditioner energy usage and its cooling/heating effect are vital. Energy usage by the air conditioner is measured by a combination of Wattnodes® and current transformers. Data acquisition hardware is placed inside of an enclosure with a dedicated power supply installed within the FEF. The data acquisition system scans the sensors multiple times a minute and records averaged values of the data onto a table every minute.

4.2 Analytical Model

A simplified analytical mathematical model was produced to validate the heat transfer measurements in the experiment. Methods to produce the model were utilized with procedures found in widely accepted literature [35,36,39]. During the summer, August 15 and 16, meteorological data were gathered as well as experimental data from the facility for a fully insulated setup. Meteorological data collected were global horizontal irradiance, direct normal irradiance, diffuse horizontal irradiance, and dry bulb temperature. Wind speed and direction data were available but the convection heat transfer on the outside of the surface was assumed to be constant for simplification. The coordinates of the facility were given as 36.11 latitude and -115.14 longitude. Tilt, azimuth and dimensions for each surface of the facility were determined. Insulation properties such as the specific heat capacity, thermal resistance, thermal conductivity, and density were obtained [40,41]. Interpolation and

extrapolation of the data were performed when necessary such as the thermal resistance shown in Figure 16. The thermal conductivity of the steel container was also determined [42].

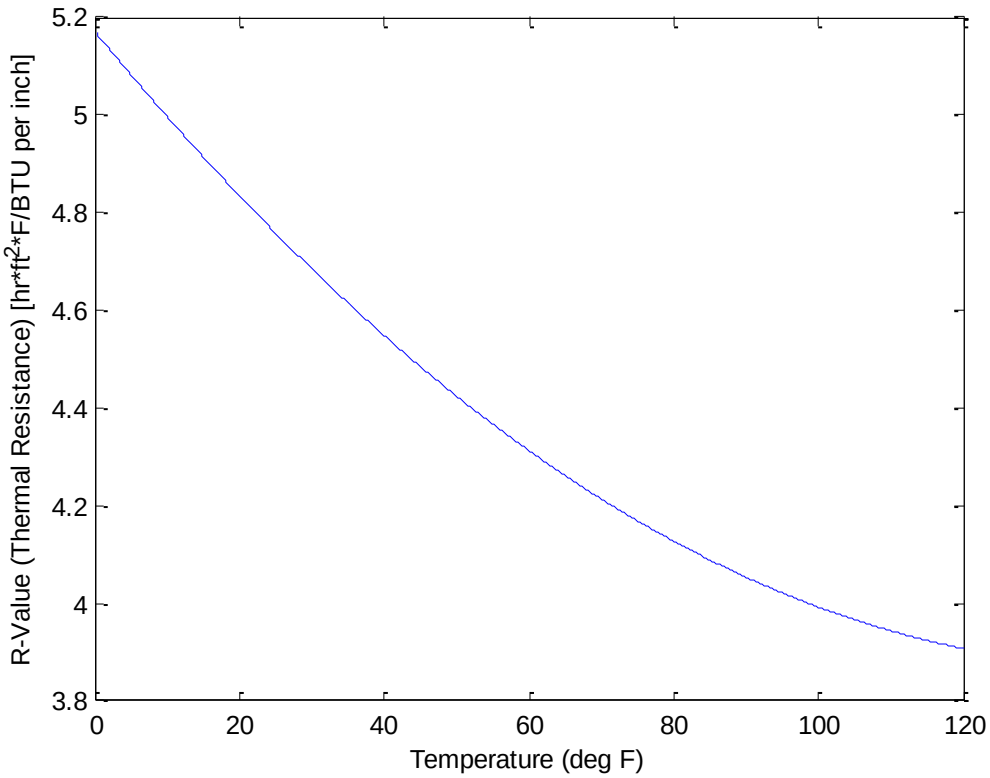

Figure 16 – R-Value of Insulation at Given Temperature

Sun angles and properties were then determined. The declination of the sun is calculated for each hour using equation (1) below.

$$\delta = (180/\pi)(0.006918 - 0.399912\cos B + 0.070257\sin B - 0.006758\cos 2B + 0.000907\sin 2B - 0.002697\cos 3B + 0.00148\sin 3B) \quad (1)$$

Where B is given as the nth day of the year in equation (2),

$$\mathrm{B} = (n-1)\frac{360}{365} \quad (2)$$

The equation of time is approximated with the following equation (3) expressed in minutes.

$$\mathrm{ET} = 2.2918(0.0075 + 0.1868\cos \mathrm{B} - 3.2077\sin \mathrm{B} - 1.4615\cos 2\mathrm{B} - 4.089\sin 2\mathrm{B}) \quad (3)$$

Local standard time (LST) and local standard meridian pacific (LSM) were required to determine the apparent solar time (AST) shown in (4).

$$\mathrm{AST} = \mathrm{LST} + \frac{\mathrm{ET}}{60} + \frac{LON - LSM}{15} \quad (4)$$

The hour angle (ω) was calculated using the apparent solar time and is shown in (5).

$$\omega = 15(\mathrm{AST} - 15) \quad (5)$$

Solar altitude and zenith angle were calculated using equation (6) and (7). Where L is the latitude, δ is the declination, and ω is the hour angle.

$$\theta_z = \cos^{-1}(\cos L\cos\delta\cos\omega + \sin\phi\sin\delta) \quad (6)$$

$$\beta = \sin^{-1}(\cos L\cos\delta\cos\omega + \sin\phi\sin\delta) \quad (7)$$

The solar azimuth angle, ϕ, were then determined using equations (8) and (9).

$$\phi = \cos^{-1}(\cos\omega\cos\delta\sin L - \sin\delta\cos L)/\cos\beta \quad (8)$$

$$\phi = \sin^{-1}(\sin H \cos\delta / \cos\beta) \quad (9)$$

The surface solar azimuth, γ, defined as the angular difference between the solar azimuth and the surface azimuth, ψ, was then calculated with equation (10).

$$\gamma = \phi - \psi \quad (10)$$

The angle between the line normal to the surface experiencing radiation and the earth-sun line is called the angle of incidence, θ. This affects the intensity of the direct component of solar radiation striking the surface. The angle of incidence was calculated in equation (11). Where, Σ, is the slope of the surface.

$$\theta = \cos^{-1}(cos\beta \cos\gamma \cos\Sigma + \sin\beta \cos\Sigma) \quad (11)$$

Radiation components are now calculated with the surface beam irradiance calculated using the straightforward geometric relationship shown in equation (12). This is only valid when $\cos\theta$ is greater than zero, else the surface beam irradiance is zero.

$$E_{t,b} = E_b \cos\theta \quad (12)$$

For the diffuse irradiance component, for vertical surfaces, the ratio of Y, of clear-sky diffuse irradiance on a vertical surface to clear-sky diffuse irradiance diffuse irradiance on the horizontal is a function of the angle of incidence shown with equations (13) and (14).

$$E_{t,d} = E_d Y \quad (13)$$

$$Y = \max(0.45, 0.55 + 0.437\cos\theta + 0.313\cos^2\theta) \quad (14)$$

For non-vertical surfaces with a given slope, the simplified relationships for the following cases are given in equations (15) and (16).

$$E_{t,d} = E_d(Y \sin\Sigma + \cos\Sigma) \;\; if\; \Sigma \leq 90° \tag{15}$$

$$E_{t,d} = E_d Y \sin\Sigma \;\; if\; \Sigma > 90° \tag{16}$$

For the ground reflected irradiance component for surfaces at any orientation is given by equation (17). Where the ground reflectance is given as ρ_g and was assumed to be constant at 0.3 for dry bare ground and desert.

$$E_{t,r} = (E_b \sin\beta + E_d)\rho_g \frac{1 - \cos\Sigma}{2} \tag{17}$$

The total surface irradiance is the sum of all these irradiance components. Irradiance on every surface of the facility was calculated including the floor. The radiation properties of the surface were then gathered such as the absorptivity of the surface, α, and the hemispherical emittance of surface, ε. The interior properties were assumed to be constant at the desired temperature condition of 25°C (77°F). Convective heat transfer coefficient for the outside surface was assumed constant while the radiation heat transfer coefficient was a function of the outside surface temperature. The convection and radiation heat transfer coefficients were combined giving a heat transfer coefficient as h. The difference between the long wave radiation incident on the surface from the sky and surroundings and radiation emitted by the blackbody outdoor temperature was assumed to be zero for a vertical surface and a constant for a horizontal surface. With the outside temperature given as t_o, this gives the heat flux into an exterior sunlit surface to be equation (18). Surface temperature is given as t_s.

$$\frac{q}{A} = \alpha E_t + h_o(t_o - t_s) - \epsilon \Delta R \tag{18}$$

Assuming the heat flux can be expressed in terms of sol-air temperature, $t_{e,}$ the equation can be given in the following equations for sol-air temperature and heat flux.

$$t_e = t_o + \frac{\alpha E_t}{h_o} - \frac{\epsilon \Delta R}{h_o} \tag{19}$$

$$\frac{q}{A} = h_o(t_e - t_s) \tag{20}$$

Using the flux and taking into account the thermal storage retained in the facility from the thermal properties of the insulation, the total conduction heat transfer through the surfaces was calculated. Each surface flux is multiplied by the corresponding surface area and summed together to give the results shown in Figure 17. The model and the experimental results show good agreement but since the model contains assumptions and simplifications the accuracy cannot be exact. The purpose was to determine whether the experimental results and mathematical model were of the same order and the figure more than represents that.

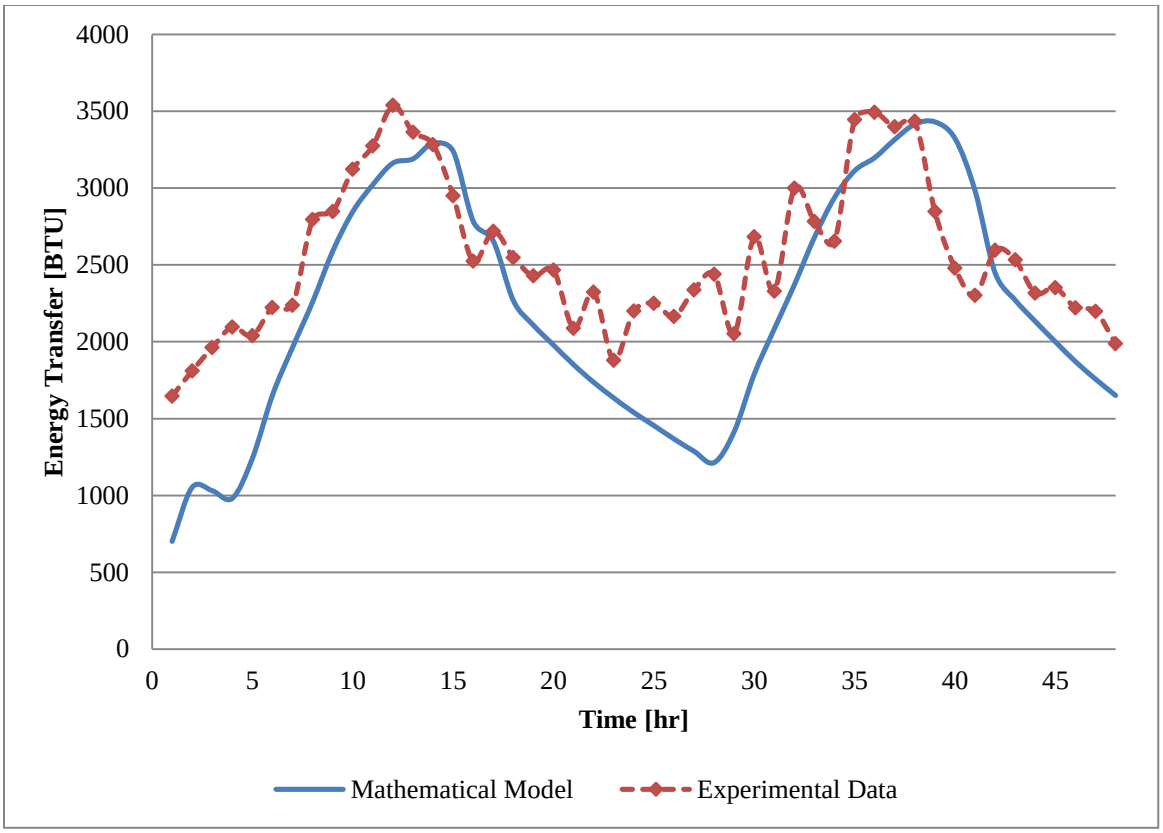

Figure 17 - Mathematical Model vs. Experimental Data Comparison for Fully Insulated Calibration Setup

4.3 Calibration

During the summer climate, testing of the fully insulated setup was performed to calibrate the experiment. The air conditioning unit maintained a desired temperature of 77°F. Results from this setup will determine how much heat enters into the container without a window installed. The approach of determining the overall heat gain was compared with the methods described by the American Society of Heating, Refrigerating and Air-Conditioning Engineers

(ASHRAE) [43]. The sensible and latent heat transfer conveyed by air on a volumetric basis are shown in equations (21) and (22).

$$q_s = C_s Q\ \Delta t \tag{21}$$

$$q_l = C_l Q\ \Delta W \tag{22}$$

For the sensible heat transfer rate, C_s is described as the air sensible heat factor, Δt is the air temperature difference across the process, and Q is the air volumetric flow rate. In the case of the latent heat transfer rate, C_l is described as the air latent heat factor, ΔW is the air humidity ratio difference across the process. The estimated values required the air flow rate data from the air conditioner. Inside and outside temperature measurements were used including the humidity measurements. Using the equations, the energy transfer estimated was calculated during a period of time in the summer. The estimated energy transfer was compared to the measured values at the same time period. The measured values consisted of using the heat flux sensors and the measured inside surface area. The measurements were conducted on a summer day and are shown in Figure 18. The figure displays a good approximation of the energy transfer.

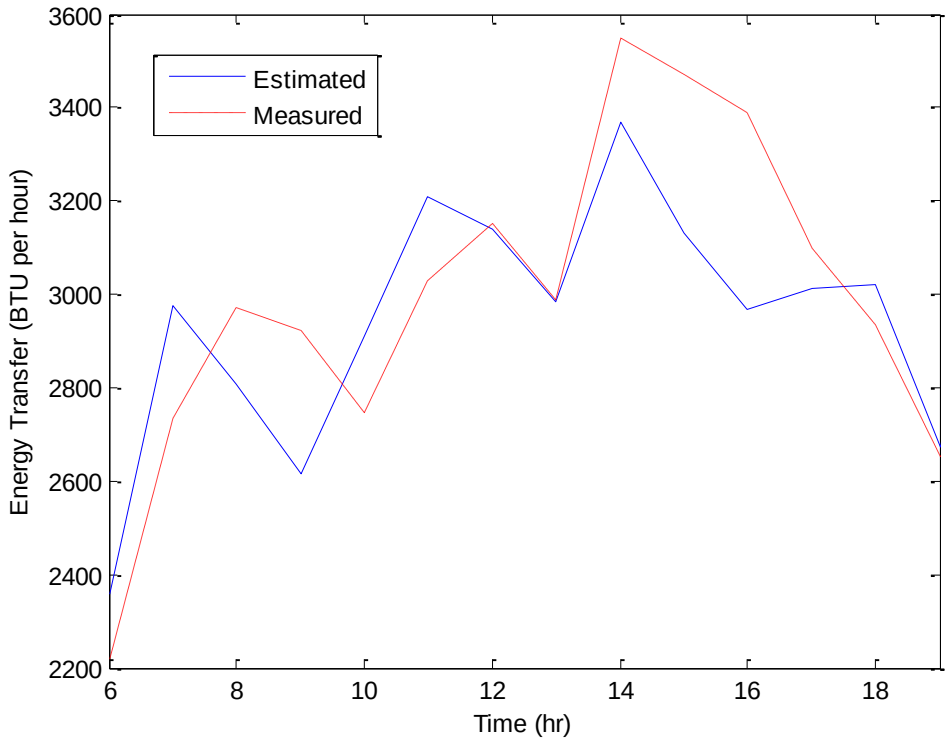

Figure 18 - Energy Transfer Comparison between Estimated and Measured Values

4.4 EER Correlation

After comparing the measured heat gain within the facility with the mathematical model and the sensible and latent heat transfer conveyed by air on a volumetric basis, analysis of the air conditioner proceeded. Energy efficiency ratio (EER) is defined as the ratio of the cooling capacity in Btu/h to the power input value in Watts at any given rating conditions expressed in Btu/Wh according to the American National Standards Institute (ANSI). Seasonal energy efficiency ratio (SEER) is the total heat removed from the conditioned space during the

annual cooling season divided by the total electrical energy consumed by the air conditioner during the same season [44].

The energy efficiency ratio of the air conditioner during the summer months was plotted versus the temperature difference between the average interior temperature and the outside air temperature as shown in Figure 19. The temperature difference is shown in degrees Celsius. The EER of the air conditioning unit increased as the temperature difference decreased. The overall seasonal energy efficiency ratio was about 16 for the particular unit during the few months in the summer period while in the fully insulated setup. Higher values of temperature difference show more consistency in EER values as would be expected. When the temperature difference is low, other factors such as solar radiation and wind speed may have influence which may cause the scattering.

After running the fully insulated setup for several months, data were gathered for the energy efficiency ratio of the air conditioning unit. The following data were then plotted against the temperature difference between the inside of the facility and the ambient temperature conditions outside of the facility. This is shown in Figure 19.

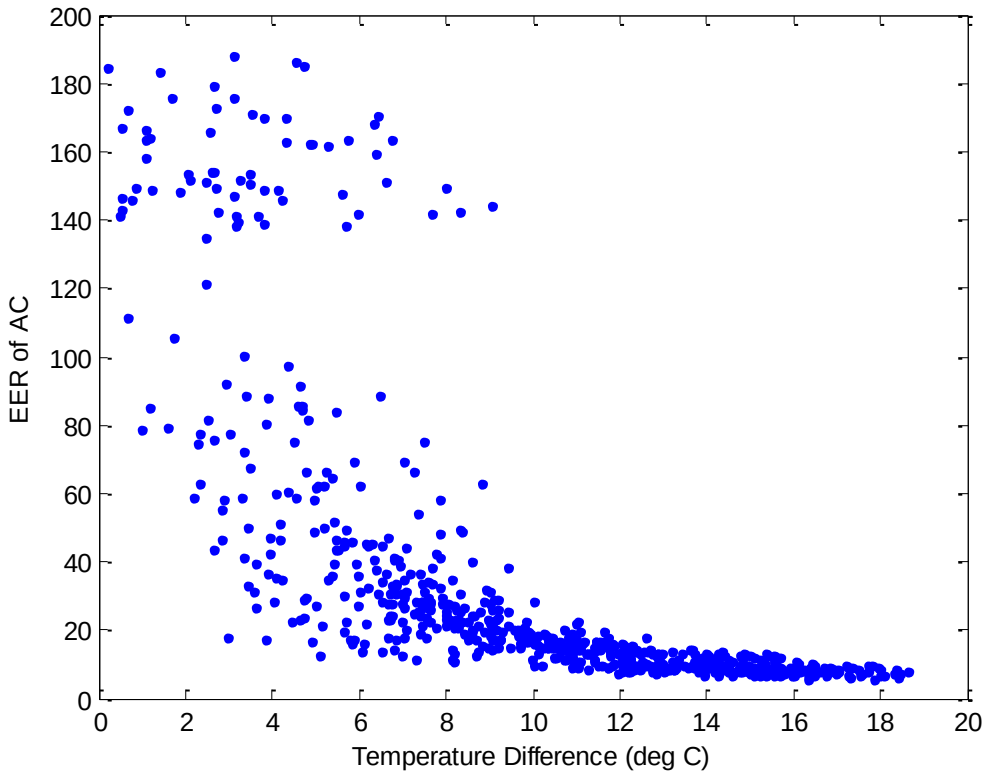

Figure 19 - Energy Efficiency Ratio for given Temperature Difference (Δ°C)

With the usage of built-in functions in MATLAB, a polynomial curve fitting was employed to determine the best curve fit for the data. After running different methods, it was found that a fifth order polynomial curve fitting fit best with the data within the given ranges.

The coefficients of the polynomial given as *p(x)* of the degree given as *n* that fits the data *p(x(i))* to *y(i)* in a least squares sense. This gives the resulting *p* as a row vector of a length n+1 that contains the polynomial coefficients in descending power shown in equation (23).

$$p(x) = p_1 x^n + p_2 x^{n-1} + \cdots + p_n x + p_{n+1} \tag{23}$$

The coefficients of the polynomial curve fitting are given as 0.00029, -0.016, 0.31, -1.50, -16.88, and 160.56. It is now possible to estimate the amount energy efficiency ratio at a given temperature difference although due to the scattering of data it is not ideal. Figure 20 shows the curve fitting at the fifth order polynomial with a temperature difference of zero to twenty in small increments.

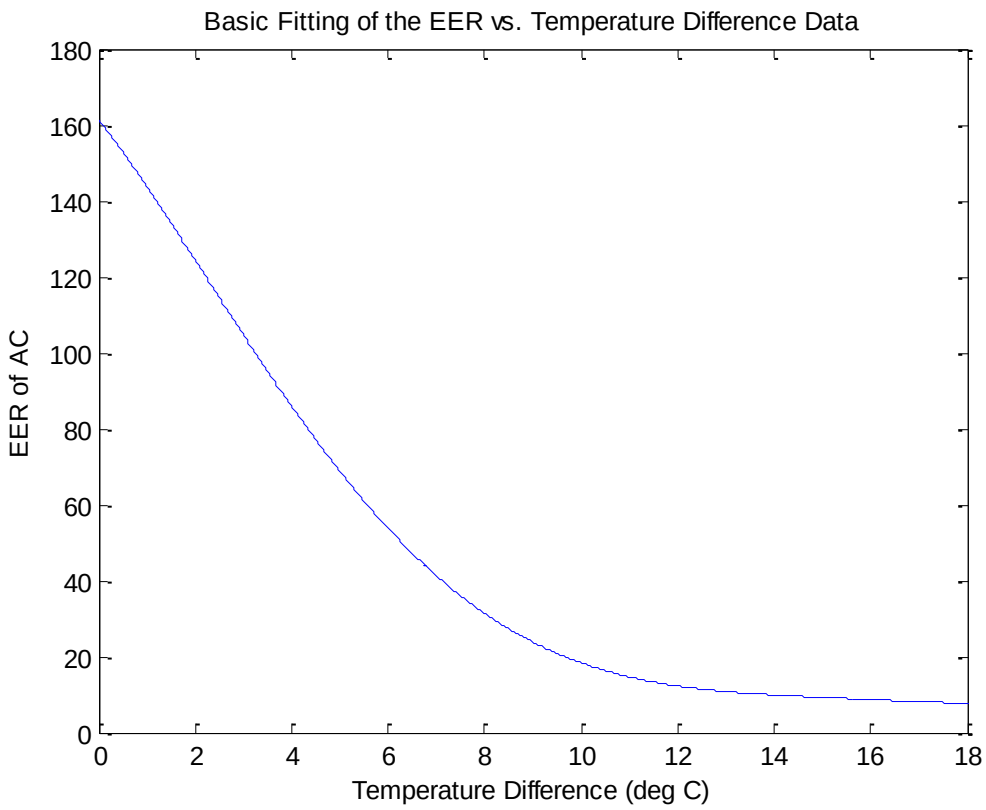

Figure 20 - Basic Fitting of the EER for given Temperature Difference Data

4.5 Uncertainty Analysis

Uncertainty analysis was performed for the instrumentation that measured the energy transfers through the window. The heat flux and pyranometer sensors were mainly targeted. Interpolation error, or zero-order uncertainty were accounted for the measurement of the inside surface areas, the heat flux and pyranometer resolutions. Instrumentation uncertainty was determined from the product specifications provided by the manufacture. Using methods

described in widely accepted literature, the uncertainty was determined using equation (24) [45,46].

$$u_R = \left[\left(\frac{\partial R}{\partial x_1}u_1\right)^2 + \left(\frac{\partial R}{\partial x_2}u_2\right)^2 + \cdots + \left(\frac{\partial R}{\partial x_n}u_n\right)^2\right]^{\frac{1}{2}} \quad (24)$$

Where,

u_R = uncertainty in the experimental results

R = given function of the independent variables, x_1, $x_2 \ldots x_n$

$u_1, u_2, \ldots u_n$ = uncertainty in the independent variables

Considering the uncertainty from each measurement of the devices and using the above equation the overall measurement uncertainties were estimated and the results are plotted in Figure 21. As shown in the figure the uncertainty decreased at higher heat transfer rates through the window and is stabilized.

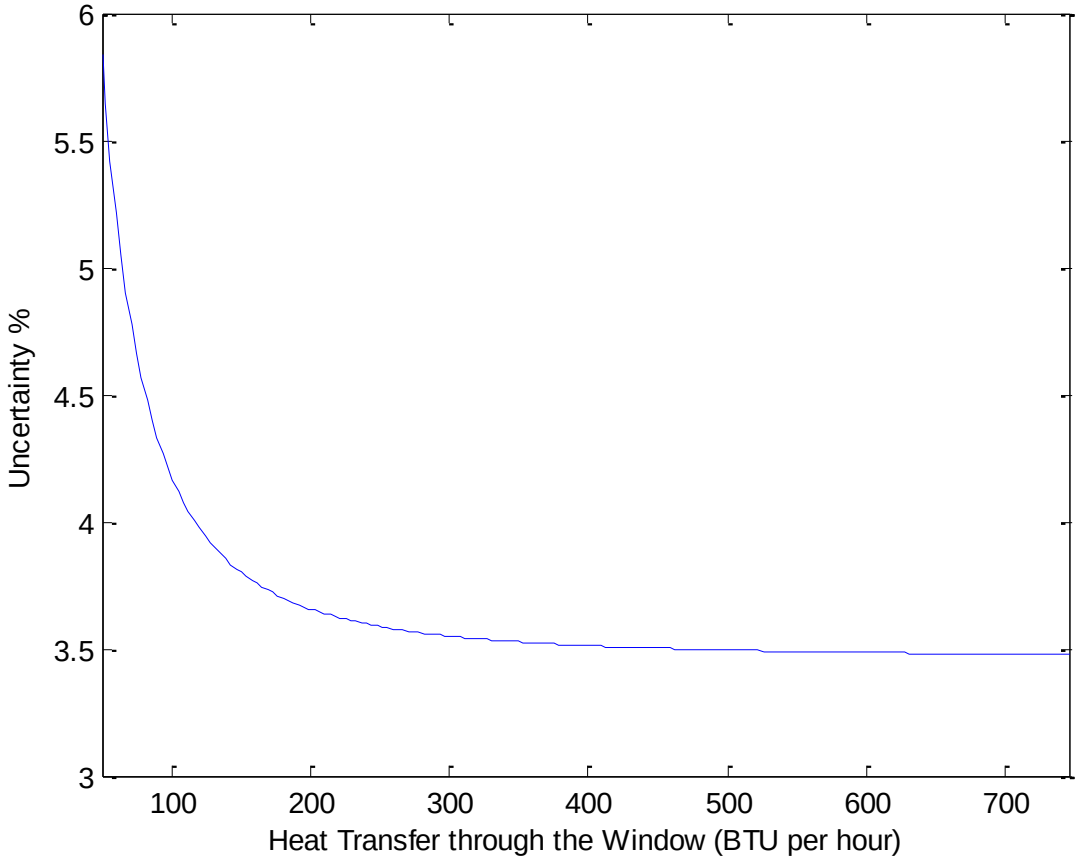

Figure 21 –Variation of Uncertainty for Heat Transfer through the Window

Chapter 5: Results and Discussion

5.1 Fenestration Value Comparisons

Two window configurations were tested with one being a standard double paned window that was easily accessible and another being a triple pane window requiring a special order to be made. The double pane window is JELD-WEN 400 series and contains a clear pane and a pane with low-e 366 glazing. The spacing between the panes is filled with argon gas. The south facing window was tested for several weeks at a time during the summer months of July through September with clear skies in Las Vegas (with latitude of 36.1°). The window has an area of 4 ft. by 4 ft. and is a typical double glazed window commonly found in US residential settings. Figure 22 shows the double-paned window testing configuration installed onto the outside of the facility. The window had a manufacturer specified solar heat gain coefficient of 0.23 and a U-Factor of 0.30 in U.S./I-P units provided by the manufacturer.

Figure 22- Double-Paned Window Setup

The triple-paned window was purchased and assembled from Davis glass (a local glass company) and also had an area of 4 feet by 4 feet (1.49 sq. m). This window consisted of two clear tempered glass panes and one single Sungate 500 glazing with low-e. Two air-gap spaces exist within the glass panes. This configuration is shown in Figure 23. This window was not a typical prebuilt window and as such did not come with a frame unless desired.

Figure 23 – Triple-Paned Window Setup

The experimental data for the window glazing were compared with a popular publically available program used for heat transfer analysis using methods consistent with the updated rating procedure developed by the National Fenestration Rating Council (NFRC) that is consistent with the ISO 15099 standard is called WINDOW and was developed by the Lawrence Berkeley National Laboratory (LBL). It is a widely accepted program and the comparisons of the experimental data are shown in Table 6. Calculations made by the

program were determined at conditions where the inside air temperature was about 75°F (24°C) and with an outside air temperature of about 90°F (32°C) for the summer period. The condition for the amount of global solar radiation is given as 248 Btu/h-ft^2 (783 W/m^2). Averaged samples of the experimental data at these conditions were used to determine the comparison values found in the table. The values for the triple-paned window are in good agreement with the Window 6.3 evaluation. Testing during the double-paned window presented larger errors in the U-factor. It was found that during testing water condensation was found inside the gap in between the double-paned window suggesting that the argon filled gap seal was compromised, thus releasing the argon within. This was changed in the Window 6.3 program to represent the gap as filled with air. Values shown for the double pane window were in good agreement when considering the air gap. It is worth noting that the low-e glazing on the triple-paned unit performed worse than the glazing found on the double-paned glazing while a slight increase in U-factor performance was seen.

Table 6 – Window 6.3 Fenestration Calculated Values Compared to FEF Fenestration Experimental Values of Window Glazing

Window	Solar Heat Gain Coefficient from Window 6.3	Solar Heat Gain Coefficient from FEF	U-Factor (Btu/h-ft^2-F) from Window 6.3	U-Factor (Btu/h-ft^2-F) from FEF
Jeld-Wen Series 400 Double-Paned Window with Argon Gas	0.28	0.25 ±0.02	0.33	0.41 ±0.02
Jeld-Wen Series 400 Double-Paned Window with Air Gap	0.28	0.25 ±0.02	0.41	0.41 ±0.02
Triple-Paned Window with Sungate Low-e and Air Gap	0.60	0.56 ±0.04	0.37	0.38 ±0.02

5.2 Building Energy Simulations

In an effort to quantify the results in the form of energy loads, building energy simulations were performed. A building energy simulation program called Energy-10 developed by the National Renewable Energy Laboratory (NREL) was used to run building energy simulations of a typical code-standard home [47]. This also presents the results in a more practical and applicable manner.

The 1,800 square feet floor area reference building was two stories. Construction of the wall consisted of a standard 2x4 timber frame construction, softwood frame, sheathing, fiberglass insulation, and drywall. Roof construction is similar to the wall construction but with increased frame thickness and insulation. Several different sizes of double-paned windows

were used. There are a total of 19 windows evenly distributed around the reference home. The total window gross area for the residential home is 300 square feet (27.9 sq. m) whereas the total wall gross area is 2,762 square feet (256.6 sq. m).

A four-person household was assumed with occupancy profile set up for a typical residential home provided by Energy-10. For comparison purposes a direct expansion cooling with gas furnace HVAC system was selected and auto sized by the program with a continuous HVAC schedule, and no setback temperatures. Other assumptions include the main entrance facing south, no added thermal mass, and an unconditioned garage space. Remaining required parameters were taken as default settings in the program. The cooling and heating requirements were found from these simulations. Figure 24 shows the cooling demand load for a building using JELD-WEN double-paned windows with the air gap. Other results include the hourly solar gains, hourly envelope conduction gains, the total net zone cooling load, which includes ventilation requirements (sensible and latent) were determined.

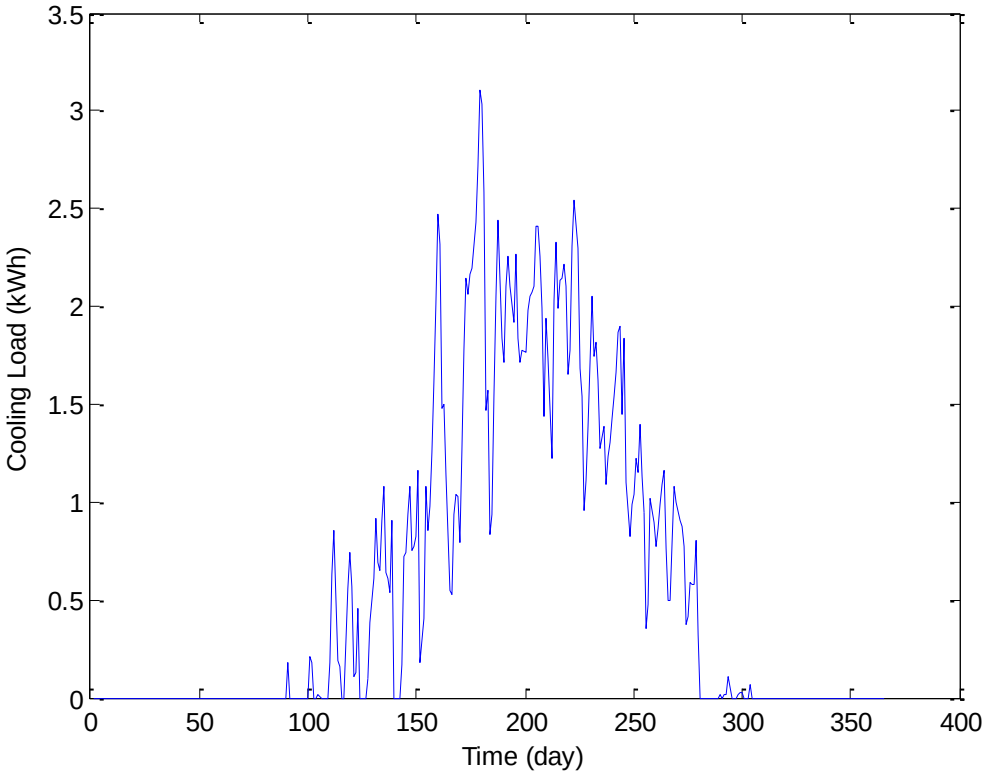

Figure 24 – Building Energy Simulation of Cooling Load Requirements for a Code Standard Home in Las Vegas, NV

Comparison of the facility heat transfer through a 4x4 window to the building energy simulation calculation of heat transfer through a 4x4 window for the summer months show good agreement. For the yearly simulation, the building energy simulation utilizes typical meteorological year (TMY) data and hence uses data from several different years to best represent the meteorological conditions at the given time [48].

Comparison between a standard double-paned window and the experimental values of the JELD-WEN window has been performed using the fenestration data shown in Table 7. The standard double-paned window in the building energy simulation has a U-factor of 0.65 Btu/h-ft^2-F and a SHGC 0.40. The table shows the solar gains, conduction gains and overall cooling electrical load for each building simulation. No shading apparatus was considered and only summer months were evaluated. The overall benefits due to JELD-WEN compared to standard double-paned window are shown. The benefits show the importance of choosing the correct windows for the climate.

Table 7 – Influence of Window Fenestration Properties on Building Energy during the Summer Period

	Jeld-Wen Series 400 Double-Paned Window with Air Gap (U-Factor: 0.41 Btu/h-ft^2-F, SHGC:0.25)	Standard Double-Paned Window with Low-E Glazing in Energy-10 Program (U-Factor: 0.65 Btu/h-ft^2-F, SHGC:0.40)	Percent Reduced Comparing Jeld-Wen with Standard Window
Solar Heat Gain (MMBTU)	5.91	11.86	50.15 %
Envelope Conduction Gain (MMBTU)	7.37	9.29	20.70 %
Cooling Load (MWh)	4.33	5.06	14.48 %

Direct benefits of reduced solar heat gain coefficients are experienced during the summer period, but this also equates to reduced heat gain during the winter months thus increasing the space heating load. From the building energy simulation the JELD-WEN windows

required 45.92 MMBTU thermal heating energy when compared to the standard window which only needed 44.22 MMBTU. This presents a 3.9% increase. To maximize the benefits of each period, an active façade may be implemented to allow more solar heat gain during the winter and reducing solar heat during the summer. For more accessible applications, the fenestration properties will be analyzed to determine the optimal characteristics for this climate.

Recommendations from Energy Star state that for the Las Vegas climate, a value of less than or equal to 0.30 for both the U-Factor (Btu/h-ft^2-F) and SHGC are ideal [49]. This value will be used as the baseline. Adjusting the SHGC with the U-Factor fixed at 0.30, the effects of SHGC on annual heating and cooling loads can be seen in Figure 25.

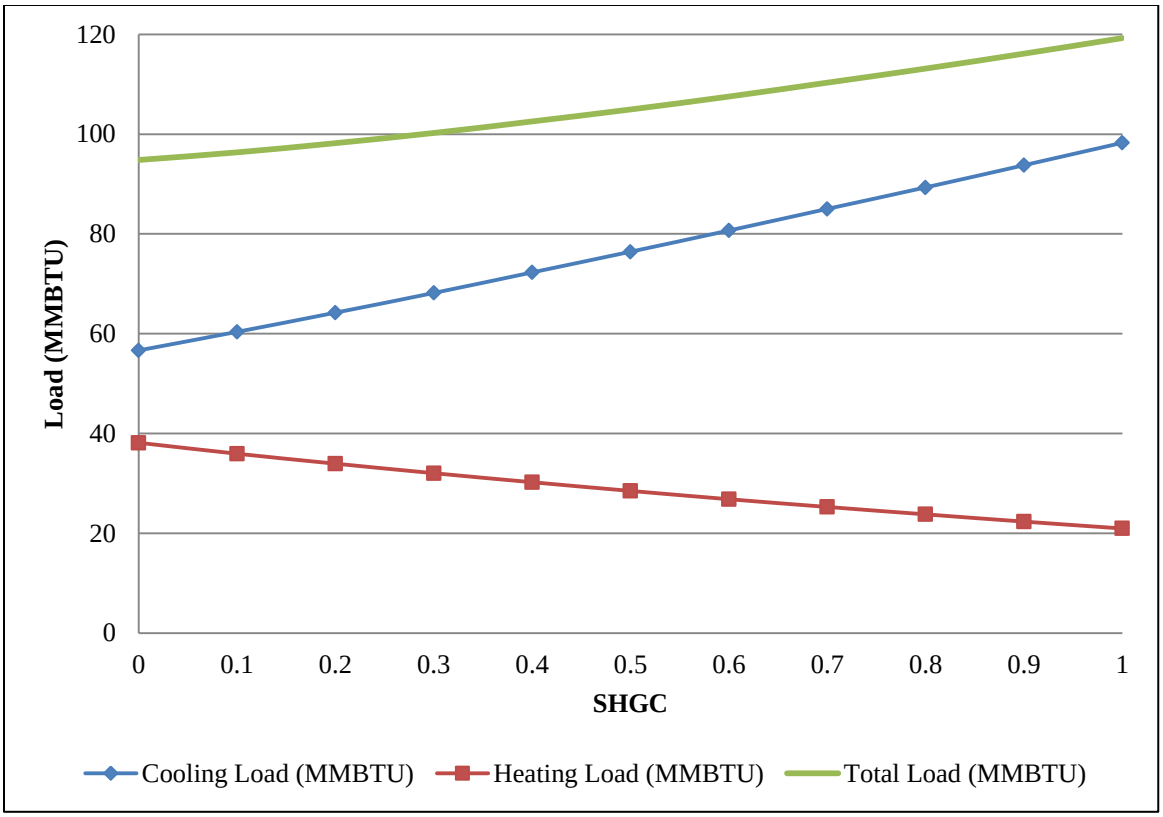

Figure 25 - Effects of SHGC on Annual Heating and Cooling Loads

As stated earlier, the heating load increases as SHGC decreases due to reduced solar energy transmission into the building during winter periods. The cooling load experiences the opposite effect, having reduced cooling loads as SHGC decreases. Although the increased heating load is undesirable, the total overall heating and cooling load manages to decrease as SHGC decreases. This is due to the cooling dominant nature for homes in the Las Vegas climate. More cooling days exists than heating days, thus the reduction of SHGC is beneficial annually.

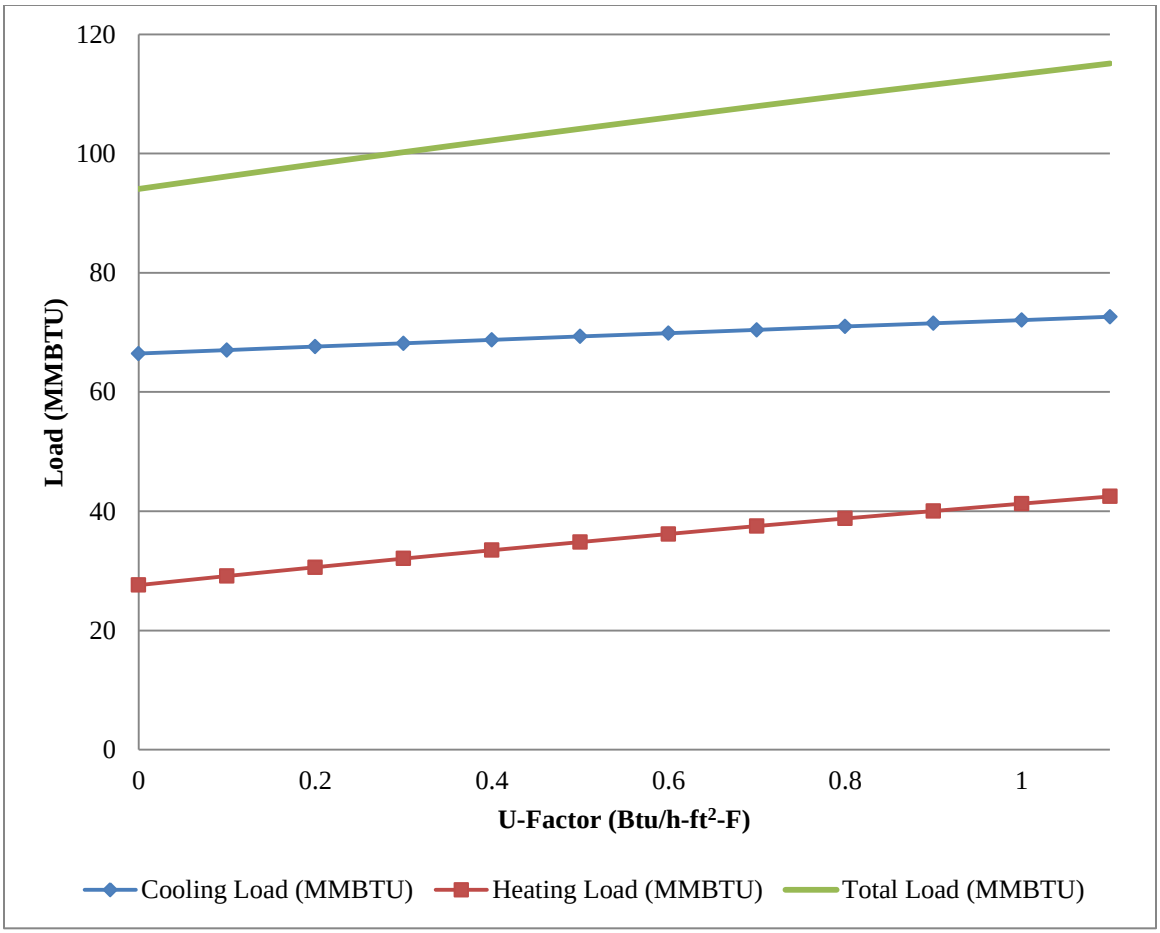

Figure 26 - Effects of U-Factor on Annual Heating and Cooling Loads

Figure 26 displays the effects of U-factor on annual heating and cooling loads. As U-factor decreases, both the heating and cooling loads decrease. The heating load experiences the most benefit due to a larger slope. Total overall cooling and heating load is reduced which is expected since the lowered U-factor provides additional improved insulation for the house, therefore reducing conduction heat transfer from the exterior into the interior. In summary,

reducing both the SHGC and the U-factor provides an annual reduction in total cooling and heating loads.

From the building conditions given previously, a fitting of the data can provide an equation that can be utilized to predict the total cooling loads with respect to either the U-factor or SHGC. Dividing by the total window area presents the results in a per square feet basis. When the SHGC is fixed at 0.30 and disregarding loads from other sources, equation (25) can be used to estimate the effects of U-factor in regards to total annual loads.

$$L = 0.94U^3 - 7.4U^2 + 71U + 0.00068 \quad (25)$$

Where L is the total annual cooling and heating loads through the window in kBTU/ft^2 and U is the U-factor given in Btu/h-ft^2-F. Similarly, for the SHGC, an equation can be produced from the fitting of the data with the U-factor fixed at 0.30 Btu/h-ft^2-F. This is seen in equation (26), and can be used to predict the effects of the SHGC on the total annual loads.

$$L = -11S^3 + 43S^2 + 49S - 0.08 \quad (26)$$

Where L is the total annual cooling and heating loads through the window in kBTU/ft^2 and S is the SHGC. These equations depend on window location and as such can only be used as a general estimation.

5.3 Facility Improvements

System improvements include creating a secondary facility to test a reference case and run experiments simultaneously in order to have a more direct relationship between different facades and windows.

Chapter 6: Conclusion

The Façade Evaluation Facility was developed for testing various types of facades at any given orientation. Removable façade configurations allow testing specimens to be changed effortlessly. The fenestration properties have been evaluated for an energy efficient double-paned window and a basic triple-paned window. Building energy simulations help demonstrate the importance of fenestration characteristics affecting building energy use. Further testing of different types of windows will continue and comparisons can be inferred between specimens. The facility allows for testing of several types of glazing, exterior cladding, building integrated photovoltaic cells and wall materials. Development of the data will help provide valuable information for energy efficient building design and sustainability.

References

[1] Yilmaz Z., 2007, “Evaluation of energy efficient design strategies for different climatic zones: Comparison of thermal performance of buildings in temperate-humid and hot-dry climate,” Energy and Buildings, 39(3), pp. 306-316.

[2] Jacobsson S., and Lauber V., 2006, “The politics and policy of energy system transformation—explaining the German diffusion of renewable energy technology,” Energy Policy, 34(3), pp. 256-276.

[3] Environmental Information Administration, 2008, “International Energy Outlook 2008,” U.S. Department of Energy.

[4] Department of Energy (DOE) Energy Efficiency and Renewable Energy (EERE), 2004, Building America puts residential research results to work, National Renewable Energy Lab., Golden, CO (US).

[5] Pérez-Lombard L., Ortiz J., and Pout C., 2008, “A review on buildings energy consumption information,” Energy and Buildings, 40(3), pp. 394-398.

[6] Lee E., Selkowitz S., Bazjanac V., Inkarojrit V., and Kohler C., 2002, “High-performance commercial building facades,” Building Technologies Program, Lawrence Berkeley National Laboratory, June 2002.

[7] Carmody J., Selkowitz S., Lee E., Arasteh D., and Willmert T., 2004, Window systems for high-performance buildings, WW Norton.

[8] Clarke J. A., Hand J. W., Johnstone C. M., Kelly N., and Strachan P. A., 1996, "Photovoltaic-integrated building facades," Renewable Energy, 8(1-4), pp. 475-479.

[9] Bazilian M. D., Leenders F., Van der Ree B. G. C., and Prasad D., 2001, "Photovoltaic cogeneration in the built environment," Solar Energy, 71(1), pp. 57-69.

[10] Krauter S., Araújo R. G., Schroer S., Hanitsch R., Salhi M. J., Triebel C., and Lemoine R., 1999, "Combined photovoltaic and solar thermal systems for facade integration and building insulation," Solar Energy, 67(4-6), pp. 239-248.

[11] Yun G. Y., McEvoy M., and Steemers K., 2007, "Design and overall energy performance of a ventilated photovoltaic façade," Solar Energy, 81(3), pp. 383-394.

[12] McGraw-Hill Construction., 2008, "Key trends in the European and US construction marketplace," SmartMarket Report. New York City: McGraw-Hill Construction.

[13] Banfi S., Farsi M., Filippini M., and Jakob M., 2008, "Willingness to pay for energy-saving measures in residential buildings," Energy economics, 30(2), pp. 503–516.

[14] Lawrence Berkeley Laboratory, 2011, WINDOW (Version 6.3) [Software], http://windows.lbl.gov/software/window/6/index.html.

[15] Baker J., Sullivan H., and Wright J., 1989, "A study of pane spacing in glazing systems," Proceedings of the Solar Energy Society of Canada, pp. 267–272.

[16] Kee M. S., Hughes D. R., Lee A. M., McMillan M., and Plewa J. E., 2010, "Capstone Design: Energy Efficient Windows Triple Pane Window Analysis," University of Tennessee Honors Thesis Projects.

[17] Reilly S., Arasteh D., and Selkowitz S., 1991, "Thermal and optical analysis of switchable window glazings," Solar Energy Materials, 22(1), pp. 1-14.

[18] Arasteh D., Selkowitz S., and Wolfe J., 1989, "The design and testing of a highly insulating glazing system for use with conventional window systems," Transactions of the ASME: Journal of Solar Energy Engineering, III, pp. 44-53.

[19] Arasteh D., 2008, "Highly insulating glazing systems using non-structural center glazing layers," 2008 Annual ASHRAE Meeting, Salt Lake City, UT, June 21-25, 2008.

[20] Klassen M. S., Sutula J. A., Holton M. M., Roby R. J., and Izbicki T., 2006, "Transmission Through and Breakage of Multi-Pane Glazing Due to Radiant Exposure," Fire Technology, 42, pp. 79-107.

[21] Citherlet S., Di Guglielmo F., and Gay J.-B., 2000, "Window and advanced glazing systems life cycle assessment," Energy and Buildings, 32(3), pp. 225-234.

[22] Xian de F., 2000, "A Study of the U-Factor of the Window with a High-Reflectivity Venetian Blind," Solar Energy, 68(2), pp. 207-214.

[23] Xiande F., 2001, "A study of the U-factor of a window with a cloth curtain," Applied Thermal Engineering, 21(5), pp. 549-558.

[24] Klems J. H., 1988, U-values, solar heat gain, and thermal performance: Recent studies using the MoWitt, Lawrence Berkeley Laboratory.

[25] Klems J. H., Selkowitz S., and Horowitz S., 1982, "A mobile facility for measuring net energy performance of windows and skylights," Proceedings of the CIB W.

[26] Klems J. H., 1988, "Measurement of fenestration net energy performance: Considerations leading to development of the mobile window thermal test (MoWitt) Facility," J. Sol. Energy Eng., 110(3), pp. 208-216.

[27] Robinson P., and Littler J., 1993, "Advanced glazing: Outdoor test room measurements, performance prediction and building thermal simulation," Building and Environment, 28(2), pp. 145-152.

[28] Baker P., and McEvoy M., 2000, "Test cell analysis of the use of a supply air window as a passive solar component," Solar Energy, 69(2), pp. 113-130.

[29] McEvoy M., Southall R., and Baker P., 2003, "Test cell evaluation of supply air windows to characterise their optimum performance and its verification by the use of modelling techniques," Energy and Buildings, 35(10), pp. 1009-1020.

[30] Baker P. H., and McEvoy M. E., 1999, "An investigation into the use of a supply air window as a heat reclaim device," Building Services Engineering Research and Technology, 20(3), pp. 105 -112.

[31] Serra V., Zanghirella F., and Perino M., 2010, “Experimental evaluation of a climate façade: Energy efficiency and thermal comfort performance,” Energy and Buildings, 42(1), pp. 50-62.

[32] University of Oregon Solar Radiation Monitoring Laboratory, “Sun path chart program,” http://solardat.uoregon.edu/SunChartProgram.html.

[33] The Center for Energy Research, “CER Data Collection,” http://www.cer.unlv.edu/cer/CERData/tabid/252/Default.aspx.

[34] National Renewable Energy Laboratory (NREL), “Daily plots and raw data files,” http://www.nrel.gov/midc/unlv/.

[35] Duffie J. A., and Beckman W. A., 2006, Solar Engineering of Thermal Processes, Wiley.

[36] American Society of Heating Refrigerating and Air-Conditioning Engineers, 2009, 2009 ASHRAE Handbook - Fundamentals (I-P) (includes CD in dual units), American Society of Heating, Refrigerating and Air-Conditioning Engineers.

[37] Incropera F. P., DeWitt D. P., Bergman T. L., and Lavine A. S., 2006, Introduction to Heat Transfer, Wiley.

[38] Concina W., Sadineni, S. B., and Boehm R. F., 2011, “Development of a façade evaluation facility for experimental study of building energy,” ASME 5th International Conference on Energy Sustainability Washington D.C.

[39] Siegel R., and Howell J., 2001, Thermal Radiation Heat Transfer 4th Edition, Taylor & Francis.

[40] Federation of European Rigid Polyurethane Foam Associations, 2006, "Thermal insulation materials made of rigid polyurethane foam," http://www.excellence-in-insulation.eu/site/fileadmin/user_upload/PDF/Thermal_insulation_materials_made_of_rigid_polyurethane_foam.pdf.

[41] Insulfoam LLC, 2008, "Insulfoam Roofing Manual, January 2008," http://www.insulfoam.com/images/stories/pdfs/Roofing_Manual/Roofing_Manual_full.pdf.

[42] The Engineering Toolbox, "Thermal Conductivity of some common Materials and Gases," http://www.engineeringtoolbox.com/thermal-conductivity-d_429.html.

[43] ASHRAE, 2009, Fundamentals Atlanta: American Society of Heating, Air-Conditioning and Refrigeration Engineers, Inc.

[44] ANSI/AHRI, 2008, "ANSI/AHRI Standard 210-240-2008 with Addendum 1."

[45] ASME PTC 19.1, 2004, "Test Uncertainty," Test Uncertainty—Instruments and Apparatus.

[46] Figliola R. S., and Beasley D. E., 2005, Theory and Design for Mechanical Measurements, Wiley.

[47] National Renewable Energy Laboratory (NREL), Energy-10, http://www.nrel.gov/buildings/energy10.html.

[48] National Renewable Energy Laboratory (NREL), "National Solar Radiation Data Base 1961- 1990: Typical Meteorological Year 2," http://rredc.nrel.gov/solar/old_data/nsrdb/1961-1990/tmy2/.

[49] Department of Energy (DOE), Environmental Protection Agency (EPA), Center for Sustainable Building Research, Alliance to Save Energy, and Lawrence Berkeley National Laboratory, "ENERGY STAR® Windows," http://www.efficientwindows.org/energystar.cfm.

VITA

Graduate College
University of Nevada, Las Vegas

Wendell Concina

Degree:

Bachelor of Science, Mechanical Engineering, 2009
University of Nevada, Las Vegas

Thesis Title: Fenestration Studies on Building Energy Using the Façade Evaluation Facility

Publications:

Concina W., Sadineni, S. B., and Boehm R. F., 2012, "Development of an In-Situ Façade-Evaluation Facility," *35X-C8C3B7H3D6, 2nd Asian-US-European Thermophysics Conference,* Hong Kong.

Concina W., Sadineni, S. B., and Boehm R. F., 2011, "Development of A Façade Evaluation Facility for Experimental Study of Building Energy," *Proceedings of ASME 5th International Conference on Energy Sustainability,* Washington, DC, 2011.

Concina W., Sadineni, S. B., and Boehm R. F., 2011, "Solar Assisted Desiccant Cooling Simulations for Different Climate Zones," *Proceedings of ASME 5th International Conference on Energy Sustainability*, Washington, DC, 2011.

Thesis Examination Committee:

Committee Chair, Robert Boehm, Ph. D.
Committee Member, Suresh Sadineni, Ph. D.
Committee Member, Yitung Chen, Ph. D.
Graduate Faculty Representative, Yahia Baghzouz, Ph. D.